HHS Public Access

Author manuscript

Nature. Author manuscript; available in PMC 2013 April 03.

Published in final edited form as:

Nature. 2012 August 30; 488(7413): 647–651. doi:10.1038/nature11310.

Autistic-like behavior and cerebellar dysfunction in Purkinje cell *Tsc1* mutant mice

Peter T. Tsai[1], **Court Hull**[2,*], **YunXiang Chu**[2,*], **Emily Greene-Colozzi**[1], **Abbey R. Sadowski**[1], **Jarrett M. Leech**[1], **Jason Steinberg**[1], **Jacqueline N. Crawley**[3], **Wade G. Regehr**[2], and **Mustafa Sahin**[1]

[1] The F.M. Kirby Neurobiology Center, Department of Neurology, Children's Hospital Boston, Harvard Medical School, Boston, Massachusetts, USA.

[2] Department of Neurobiology, Harvard Medical School, Boston, Massachusetts, USA.

[3] Laboratory of Behavioral Neuroscience, Intramural Research Program, National Institute of Mental Health, NIH, Bethesda, MD, USA.

Autism spectrum disorders (ASDs) are highly prevalent neurodevelopmental disorders[1], but the underlying pathogenesis remains poorly understood. Recent studies have implicated the cerebellum in these disorders with post-mortem studies in ASD patients demonstrating cerebellar Purkinje cell (PC) loss[2,3], while isolated cerebellar injury has been associated with a higher incidence of ASDs[4]. However, the extent of cerebellar contribution to the pathogenesis of ASDs remains unclear. Tuberous Sclerosis Complex (TSC) is a genetic disorder with high rates of comorbid ASDs[5] that results from mutation of either *TSC1* or *TSC2*, whose protein products dimerize and negatively regulate mTOR signaling. TSC is an intriguing model to investigate the cerebellar contribution to the underlying pathogenesis of ASDs, as recent studies in TSC patients demonstrate cerebellar pathology[6] and correlate cerebellar pathology with increased ASD symptomatology[7,8]. TSC patients with ASDs also display hypermetabolism in deep cerebellar structures on functional imaging when compared to TSC patients without ASDs[9]. However, to date, *Tsc1*'s roles and the sequelae of *Tsc1* dysfunction in the cerebellum have not been investigated. Here we show that both heterozygous and homozygous loss of *Tsc1* in mouse cerebellar PCs results autistic-like behaviors, including abnormal social interaction, repetitive behavior, and vocalizations, in addition to decreased PC excitability. Treatment of mutants with the mTOR inhibitor, rapamycin, prevented the pathological and behavioral deficits. These findings demonstrate

Correspondence and requests for materials should be addressed to mustafa.sahin@childrens.harvard.edu or peter.tsai@childrens.harvard.edu..

*these authors contributed equally to this work.

AUTHOR CONTRIBUTIONS

P.T.T. and M.S. conceived of and designed the experimental approach, performed experiments, and prepared the manuscript. C.H. and Y.X.C. designed and performed cerebellar slice experiments and assisted in manuscript preparation. E.G., A.S., and J.L. assisted with behavioral experiments and statistical analysis. J.S. contributed to experimental quantification. J.N.C. provided training for behavioral phenotyping and contributed to behavioral experimental design and analysis. W.G.R. and M.S. supervised the project and contributed to experimental design and analysis.

novel roles for *Tsc1* in PC function and define, for the first time, a molecular basis for a cerebellar contribution to cognitive disorders such as autism.

To evaluate *Tsc1*'s role in cerebellar PCs, we generated mice with *Tsc1* deleted in cerebellar PCs ($L7^{Cre};Tsc1^{flox/+}$ (het) or $L7^{Cre};Tsc1^{flox/flox}$(mutant))[10]. Cre expression is high in PCs with expression noted by post natal day (P)6[11]. $Tsc1^{+/+}$ (WT), $L7^{Cre};Tsc1^{+/+}$ (L7Cre), $Tsc1^{flox/flox}$ (Flox), het, and mutant mice did not show reduced survival, and weights were comparable across genotypes, unlike the severe phenotype of neuronal or glial *Tsc* mutants (Figure Supplemental (S)1)[12].

To insure that TSC1 function was impaired in PCs, we evaluated staining of phospho-S6 (pS6) – a downstream effector of mTOR signaling. We expected TSC1 dysfunction to result in increased mTOR activity and indeed detected increased pS6 staining in het and mutant PCs (Figures S2-4). To assess the specificity of Cre-mediated recombination, we crossed $L7^{Cre}$ and *Rosa26* reporter mice and found only infrequent, scattered recombination in non-cerebellar areas as previously described (Figure S5)[11]. We also examined pS6 staining in other brain regions but found no differences between mutants and controls, except in cerebellar PCs (Figure S6).

One of the most consistent pathologic findings in post-mortem studies of ASD patients is reduced cerebellar PC numbers[2]. In the mutant cerebellum, while basic cellular architecture was maintained in adult mice, the PC layer was abnormal with increased soma area and reduced PC numbers when compared to control or het littermates (Figure 1A, S7). To investigate why PCs were decreased in mutants, we quantified PC numbers throughout development. Decreased cell numbers were first noted at 2 months of age with further reduction by 4 months of age, a reduction not seen in hets (Figure 1B). As these findings suggested cell loss, we investigated markers of apoptosis and found increased TUNEL and cleaved caspase 3 staining in mutant PCs at 7-8 weeks (Figure 1C, S8-9). Recently, neuronal stress in the cerebellum has been implicated in ASD pathogenesis[13] while studies have demonstrated critical roles for the TSC/mTOR pathway in mediating neuronal stress responses[14,15]. To investigate whether similar mechanisms were involved in *Tsc1* mutant PC death, we evaluated markers for both ER (GRP78) and oxidative (Heme Oxygenase 1) stress and found significantly elevated levels of both markers (Figure S9).

As TSC-mTOR signaling plays important roles in neuronal morphology/function[16,17], we also investigated whether *Tsc1* loss resulted in morphological changes in PCs at 4 weeks. TSC has known roles in the regulation of cell size[17,18], and PC soma area was significantly increased in mutant, but not het, mice (Figure 1D, S10). TSC has also been implicated in regulating dendritic spine numbers[19], and we found increased spine density on het and mutant PC dendrites (Figure 1D, E). Interestingly, decreased spine density has been reported in hippocampal and cortical neurons with *Tsc* loss[17,19,20], suggesting diverse mechanisms underlying TSC1/2's regulation of dendritic spines. We also found numerous axonal varicosities and abnormal axonal collaterals in mutants (Figure S11), consistent with known roles for TSC in regulating axonal morphology[16,21].

To investigate whether PC *Tsc1* mutants might demonstrate abnormal behaviors found in ASDs, we first evaluated social interaction, using a three chambered assay of social approach and preference for social novelty. We found social impairment in both het and mutant animals with no significant differences found between time spent in the chamber or interacting with the novel mouse versus novel object (Figure 2A). Subsequently, in a social novelty paradigm, while control animals spent significantly more time in the chamber and in close interaction with the novel animal, het, and mutant animals displayed no significant preference for social novelty by either measure (Figure 2B). We further tested whether mutants would have impaired social interaction in male – female interactions and observed significant reductions in mutant interaction time compared with controls (Figure S12).

With the cerebellum's role in motor functions, we investigated whether motor deficits contributed to social impairment. Mutants' motor activity was indistinguishable from littermates until approximately 7-8 weeks of age when mutants displayed initial signs of ataxia. Ataxia progressed and by four months there were marked changes in gait parameters (Figure S13). Hets, however, displayed no ataxia (Figure S13) and locomotion during social testing and open field testing was not significantly different between genotypes (Figure S14-15), suggesting that motor impairments were not responsible for observed social deficits.

In rodents, social interaction largely depends on olfactory cues. We observed comparable time spent investigating three non-social olfactory cues – water, almond extract, and banana extract (Figure S16), indicating that olfactory function in mutants is intact. However, consistent with observed social impairment phenotypes, het and mutant mice demonstrated reduced investigation of social odors compared to controls, suggesting that impaired discrimination of social olfactory cues contributed to social deficits in mutants.

ASD patients also display repetitive behaviors and cognitive, behavioral inflexibility. To model the perseverative thinking and cognitive inflexibility exhibited by patients with ASDs, we tested animals in a reversal learning paradigm using a water T maze. Mutant animals demonstrated similar acquisition learning of a submerged, escape platform location (days 1-3) to control littermates (Figure 2C, S17), using two measures of learning performance – correct trials and trials needed before 5 consecutive correct trials. However, when the escape platform location was reversed, mutant animals demonstrated significantly impaired learning of the new platform location. We also examined repetitive behavior in a repetitive grooming task and found significantly increased self-grooming rates in hets and mutants (Figure 2D).

ASD patients also demonstrate deficits in communication. Murine pups use ultrasonic vocalizations (USV) to communicate with their mothers, and abnormal mother-pup communication has recently been demonstrated in *Tsc2*+/- mice[22]. We evaluated USV from P5-12 and, similar to reported ASD mouse models[23], found increased vocalizations in both hets and mutants (Figure 2E). Consistent with roles for *Tsc1* in regulating these early phenotypes, pS6 levels were elevated by P7 in mutant PCs (Figure S3). Motor deficits are also found in over 50% of patients with ASDs. To evaluate whether mutants have impaired

motor learning, we evaluated mutant animals prior to ataxia onset on the accelerating rotarod and found significantly impaired motor learning in mutants (Figure S18).

The changes in PC morphology, combined with previous reports that *Tsc1* loss can alter synaptic properties[17,20], suggested that synaptic inputs to PCs might also be affected. PCs receive a single, strong climbing fiber (CF) input and many weak granule cell-parallel fiber (PF) inputs (Figure 3A). However, we found no difference in the amplitude of single fiber CF inputs between mutant and littermate controls (Figure 3B) at P28. In control animals, when synapses are stimulated twice in rapid succession, CF synapses depress, whereas PF synapses facilitate, consistent with the high and low release probabilities of these synapses, respectively (Figure 3B, left). The same characteristic plasticity was observed in mutants (Figure 3B, right). We also stimulated PFs, which produce both a direct excitatory short-latency PF EPSC and a disynaptic IPSC that arises from PF activation of molecular layer interneurons (Figure 3C, left). There was a trend towards a reduction in the ratio of the amplitudes of the EPSCs and IPSCs recorded in PCs, but it was not statistically significant (Figure 3C, right). Although it is difficult to exclude a subtle effect on synaptic properties, these results suggest that in spite of morphological differences, synaptic function in mutants appears normal.

Previous studies of *Tsc1* have also focused on neurons that are quiescent in the absence of excitatory input, whereas PCs fire spontaneous action potentials even in the absence of synaptic inputs. Because PC firing rate is thought to be critical for encoding cerebellar output in deep cerebellar nuclei (DCN)[24], we examined the intrinsic excitability of PCs using extracellular recordings, and found a significantly lower, graded spontaneous spiking rate in hets and mutants (Figure 3D, left). Moreover, also in graded fashion, current injection evoked fewer action potentials in het and mutant PCs (Figure 3E). A plot of firing frequency versus injected current shows that het and mutant PCs were significantly less excitable than controls (Figure 3E, right). Injection of small hyperpolarizing currents resulted in smaller voltage changes in mutant and het PCs suggesting a decrease in the effective input resistance (Figure S19A), which has been described previously for hippocampal neurons[17], likely contributed to the reduced excitability of PCs in mutant and het animals. By 6 weeks of age there was an even more profound reduction in excitability in mutant mice (Figure S19B). Hence, despite receiving seemingly normal functioning synaptic inputs, the output of the cerebellar cortex of het and mutant animals appears to be strongly reduced, both tonically and in response to incoming excitatory drive. Our findings implicate reduced PC excitability as a potential mechanism underlying the abnormal behaviors in PC *Tsc1* mice, consistent with clinical observations of impaired cerebellar function in ASD patients[9,25].

To evaluate whether the abnormal phenotypes seen in PC *Tsc1* mice were modifiable as demonstrated in other models of increased mTOR signaling[12,19,26], we treated animals with the mTOR inhibitor, rapamycin, starting at P7. Whereas vehicle treatment resulted in identical phenotypes to untreated cohorts, rapamycin treatment prevented the development of pathologic deficits in mutant animals, with mutant soma size and PC numbers indistinguishable from controls (Figure 4A, S20).

We subsequently evaluated whether the abnormal behaviors could also be rescued with rapamycin treatment. In vehicle treated mice, behavioral phenotypes were identical to untreated cohorts (Figure 4B-C, S21-23); however, rapamycin treatment ameliorated the motor phenotypes seen in mutant animals in gait testing and the rotarod (Figure S21, S24). Rapamycin treatment also prevented deficits in the water T Maze with no significant differences seen between rapamycin treated mutants and controls in both acquisition and reversal learning (Figure 4B, S22). In addition, following rapamycin treatment, mutants displayed comparable social behaviors to controls in both social approach and social novelty assays (Figure 4C, S23). Thus, rapamycin prevented both pathologic and behavioral phenotypes in *Tsc1* PC mutants, supporting the possibility of a therapeutic role for mTOR inhibition.

Our study demonstrates critical, novel roles for the TSC-mTOR pathway in cerebellar PCs. We find that mice with homozygous loss of *Tsc1* in PCs (mutant) demonstrated social impairment, restrictive behavior, and abnormal vocalizations – representative of the three core deficits in ASDs. Mutants also displayed pathologic features found in ASD post-mortem studies with reduced PC numbers and evidence of increased neuronal stress. While PC loss has been reported in postmortem studies of ASD patients, several lines of evidence suggest that PC death cannot fully explain the abnormal behaviors seen in PC *Tsc1* mice. Prior to PC death, mutants displayed abnormal vocalizations and motor learning impairments. In addition, mice with heterozygous loss of *Tsc1* displayed no evidence of PC loss yet displayed autistic-like behaviors.

In this study, we also demonstrate that loss of *Tsc1* from cerebellar PCs is sufficient to result in abnormal autistic-like behaviors. These findings implicate the cerebellum in the neural circuitry mediating core features of autism. The cerebellum has been previously suggested to play roles in social interaction[27] while cerebellar abnormalities are associated with ASDs as well as cognitive and behavioral disturbances[28]. How the cerebellum modulates the abnormal behaviors of autism remains a topic of intense investigation. Autism has been proposed to be a disorder of abnormally distributed networks[29]. The cerebellum, via the DCN, is connected to these networks and cortical areas implicated in ASDs. Akin to its role in motor coordination, the cerebellum has been proposed to modulate these cognitive networks, with dysfunction resulting in abnormally regulated behaviors comparable to cognitive, behavioral dysmetria[30]. Our data displayed markedly impaired PC excitability in both hets and mutants. As PC firing rates are critical determinants of DCN output, by affecting DCN activity, PC dysfunction could be postulated to alter these downstream neuronal networks, thereby contributing to abnormal autistic-like behaviors. Therefore, PC *Tsc1* mutants should provide a valuable experimental system to investigate the effects of PC dysfunction on these neuronal networks and other mechanisms contributing to the pathogenesis of ASDs.

METHODS

Mice

L7^{cre}; *Tsc1*$^{flox/flox}$ (mutant)animals were generated by crossing *L7/Pcp2-Cre* (*L7*^{Cre}) transgenic mice[11] with floxed *Tsc1* mice (*Tsc1*$^{flox/flox}$)[10] to yield *L7*^{Cre};*Tsc1* $^{flox/+}$ progeny.

These progeny were then crossed with one another or with *Tsc1*$^{flox/flox}$ animals to yield litters consisting of control (*Tsc1*$^{+/+}$ (WT), *Tsc1*$^{flox/+}$, *L7*^{Cre};*Tsc*$^{+/+}$ (L7Cre), or *Tsc1*$^{flox/flox}$(Flox)) mice, heterozygous (*L7*^{Cre};*Tsc1*$^{flox/+}$ (het)) mice, or mutant (*L7*^{Cre};*Tsc1*$^{flox/flox}$ (mutant)) mice. Only male animals were used for behavioral experiments except for ultrasonic vocalizations where both male and female pups were utilized in the analysis. Mice were of mixed genetic backgrounds (C57Bl/6J, 129 SvJae, BALB/cJ). During analysis, germline deletion was discovered to occur in the mouse colony at a frequency of ~5%. Genotyping for het mice would exclude inclusion of these animals in this cohort, but it is possible that a small percentage of *L7*^{Cre};*Tsc1*$^{flox/-}$ mice were included in the mutant cohort. As such, we repeated behavioral analysis in a cohort of mutant (*L7*^{Cre};*Tsc1*$^{flox/flox}$[LFF]) mice and littermate controls and found no significant differences with the previous mutant (LFF*) cohort (Figure S25-26), and thus cohorts were combined for analysis. As behavioral data revealed comparable behavioral phenotypes between all untreated control (*Tsc1*$^{+/+}$, *Tsc1*$^{flox/flox}$, *L7*^{Cre};*Tsc*$^{+/+}$) genotypes, these genotypes were pooled for behavioral studies involving rapamycin treatment. All experimental protocols were approved by the Animal Research at Children's Hospital Committee.

Behavioral Analysis

Social Interaction—Animals were tested for social interaction in the three chambered apparatus (Dold Labs) as previously described[31]. Time in chambers and number of crossings between chambers was recorded in an automated manner (National Instruments). Time spent interacting with the novel animal and object was recorded by the examiner with stopwatch. Animals were tested between 7-9 weeks of age. For male-female interaction, tested males were placed into an open field with control females and evaluated for male-initiated interaction over a five minute period. All behavioral assays (including social interaction) were performed by examiner blinded to genotype.

Gait Analysis—Animals were placed into the end of an apparatus 5 cm in width (preventing animals from turning around), 56 cm in length with paper placed along the entire course of the apparatus. Apparatus walls consisted of opaque material and were 15 cm in height preventing animals from looking or escaping beyond walls. Paws were painted with red (Forepaws) and black (Hindpaws) ink. Length of stride was measured from the longest stride for each trial. Stride width was also measured between hind paws at time of the longest stride. Measurements were taken from 14-16 week old animals.

Open Field—Open field testing was performed as described for 15 minute period[32]. Movement and time spent in center quadrants were recorded by video camera and analyzed by Noldus (Virginia) analysis software. Measurements were taken from animals aged 7-10 weeks.

Olfaction—Olfaction was tested as previously described[33]. Animals were presented sequentially with odors on cotton tipped applicators: first non-social, then social odors. Odors were presented in 3 consecutive trials per odorant stimulus (2 minutes/trial) in the following order: water, almond extract, banana extract, social odor 1, and lastly social odor

2. Social odors were swipes from cages containing unfamiliar, gender (male), and age matched animals. Measurements were taken from animals aged 8-12 weeks.

Grooming—After habituation, animals were observed for 10 minutes, and time spent grooming was recorded as described[34]. Measurements were taken from animals aged 8-12 weeks.

Water T Maze—Reversal learning was tested using the water T maze as described[35]. On Days 1-3, mice were given 15 trials and tasked to locate a submerged platform placed in one of the maze arms. After 15 trials on Day 3, the platform was changed to the other T arm. Mice were then tested for 15 additional trials (Reversal (R)Day1). Then for 2 subsequent days (Reversal (R)Day 2-3), mice were given 15 trials/day. Number of correct trials and number of trials required to achieve 5 consecutive correct trials were recorded. Measurements were taken from animals aged 8-12 weeks.

Ultrasonic Vocalizations—Ultrasonic Vocalizations were tested as described on postnatal days 5-12[23]. Pups were removed individually from their mother and placed inside a soundproof container where 3 detectors were used to monitor vocalizations for 5 minutes. Calls were recorded using Ultravox recording software (Noldus)[36]. Maternal genotype in all experiments was $L7^{Cre};Tsc1^{flox/+}$.

Accelerating Rotarod—Animals were tested using the Accelerating Rotarod as described over 5 consecutive days[37]. Animals were tested prior to overt ataxia between 5-7 weeks of age.

Slices: Acute sagittal slices (250-300 μm thick) were prepared from the cerebellar vermis of 4 and 6 week old mutant and control littermates. Slices were cut in an ice cold artificial cerebrospinal fluid (ACSF) solution consisting of (mM): 125 NaCl, 26 $NaHCO_3$, 1.25 NaH_2PO_4, 2.5 KCl, 1 $MgCl_2$, 2 $CaCl_2$, and 25 glucose (pH 7.3, osmolarity 310) equilibrated with 95% O_2 and 5% CO_2. Slices were initially incubated at 34° C for 25 minutes, and then at room temperature prior to recording in the same ACSF.

Recordings: Visually guided (infrared DIC videomicroscopy and water-immersion 40x objective) whole-cell recordings were obtained with patch pipettes (2-4 MΩ) pulled from borosilicate capillary glass (World Precision Instruments) with a Sutter P-97 horizontal puller. Electrophysiological recordings were performed at 31-33° C.

IPSCs were recorded at the EPSC reversal potential, and PF EPSCs were recorded at the IPSC reversal potential. To measure climbing fiber synaptic inputs, 500 nM NBQX was used to reduce the size of synaptic currents, and picrotoxin (20 μM) was used to block GABAergic inhibition. For experiments recorded at the EPSC reversal potential and for CF EPSCs, the internal pipette solution contained (in mM): 140 Cs-methanesulfonate, 15 HEPES, 0.5 EGTA, 2 TEA-Cl, 2 MgATP, 0.3 NaGTP, 10 phosphocreatine-$tris_2$, 2 QX 314-Cl. pH was adjusted to 7.2 with CsOH. Membrane potentials were not corrected for the liquid junction potential. The EPSC and IPSC reversal potentials were determined in each experiment by adjusting the membrane potential until no EPSC or IPSC was evident, and

was approximately +15 mV for the EPSC reversal, and -65 mV for the IPSC reversal. For current-clamp recordings, the internal solution contained (in mM): 150 K-gluconate, 3 KCl, 10 HEPES, 0.5 EGTA, 3 MgATP, 0.5 GTP, 5 phosphocreatine-tris$_2$, and 5 phosphocreatine-Na$_2$. pH was adjusted to 7.2 with NaOH. Current-clamp and extracellular recordings were performed in NBQX (5 μM), R-CPP (2.5 μM), and picrotoxin (20 μM) to block AMPA receptors, NMDA receptors, and $GABA_A$ receptors respectively. All drugs were purchased from Sigma-Aldrich or Tocris. Electrophysiolgical data were acquired as described previously [38].

Rapamycin Treatment: Rapamycin was dissolved in 0.25% polyethylene glycol and 0.25% tween prior to usage. Vehicle or rapamycin was administered intraperitoneally every Monday, Wednesday, and Friday with rapamycin dosed at 6 mg/kg per injection starting at P7. As behavioral data revealed comparable behavioral phenotypes between all untreated control (*Tsc1*$^{+/+}$, *Tsc1*$^{flox/flox}$, *L7*^{Cre}*;Tsc*$^{+/+}$) genotypes, these genotypes were pooled for behavioral studies involving rapamycin treatment.

Immunohistochemistry: Mice were perfused and post-fixed with 4% paraformaldehyde. Sections were prepared by cryostat sectioning and were stained with the following antibodies: PhosphoS6 (Cell Signaling), calbindin (Sigma, Cell Signaling), GRP78 (Stressgen), Heme Oxygenase-1 (Stressgen), Cleaved Caspase 3 (Cell Signaling). TUNEL staining was performed per manufacturer recommendations (Millipore).

Microscopy: Intracellular labeling of Purkinje cells was accomplished using recording pipettes filled with 0.05% biocytin (Tocris). Neurons in deeper portions of the Purkinje cell layer were targeted and filled for 3 min, and then the pipette was slowly withdrawn so that the cell membrane could reseal. Slices (250 μm thick) were then fixed in 4% paraformaldehyde in 0.1 M phosphate buffer for 24 hours, rinsed thoroughly in PBS, and incubated for 90 min in a PBS solution containing 0.5% Triton-X, 10% normal goat serum and streptavidin Alexa Fluor 488 conjugate (1:500, Life Technologies). Slices were then rinsed in PBS, mounted on Superfrost Plus slides (VWR International), air-dried, and cover-slipped in Vectashield mounting media (Vector Labs). Immunohistochemical studies were captured using Zeiss Confocal LSM710. Images were processed and morphology quantified using ImageJ software with studies performed by examiner blinded to genotypes.

Statistics: Data are reported as mean ± SEM, and statistical analysis was carried out with GraphPad Prism software using one- and two-way ANOVA with Bonferroni's multiple comparison tests for post hoc analysis unless otherwise specified.

Supplementary Material

Refer to Web version on PubMed Central for supplementary material.

ACKNOWLEDGEMENTS

We thank Gabriel Corfas, Michela Fagiolini, Paul Rosenberg, and Samuel Goldman for assistance with behavioral experiments. We are grateful to Christopher Walsh, Larry Benowitz, and members of the Sahin laboratory for critical reading of the manuscript. We are grateful to Matt Gregas for advice regarding statistical analysis. P.T.T.

received support from the Developmental Neurology Training Grant (T32 NS007473), American Academy of Neurology, and the Nancy Lurie Marks Family Foundation. This work and M.S. are supported in part by the NIH (R01 NS58956), the John Merck Scholars Fund, Autism Speaks, Nancy Lurie Marks Family Foundation, Children's Hospital Boston Translational Research Program, and the Children's Hospital Boston Mental Retardation and Developmental Disabilities Research Center (P30 HD18655). J.N.C. is supported by the Intramural Research Program, NIMH. W.G.R. is supported by the NIH (R01NS032405) and the Simons Foundation (SFARI 232304). Y.X.C. is supported by the Howard Hughes Medical Institute Medical Research Fellowship.

Financial Statement

M.S. has served as a consultant and site-PI for Novartis. He is also the PI for an investigator-initiated clinical trial partially funded by Novartis.

REFERENCES

1. Prevalence of autism spectrum disorders - Autism and Developmental Disabilities Monitoring Network, United States, 2006. MMWR Surveill Summ. 2009; 58:1–20.
2. Bauman ML, Kemper TL. Neuroanatomic observations of the brain in autism: a review and future directions. Int J Dev Neurosci. 2005; 23:183–187. [PubMed: 15749244]
3. Amaral DG, Schumann CM, Nordahl CW. Neuroanatomy of autism. Trends Neurosci. 2008; 31:137–145. [PubMed: 18258309]
4. Limperopoulos C, et al. Does cerebellar injury in premature infants contribute to the high prevalence of long-term cognitive, learning, and behavioral disability in survivors? Pediatrics. 2007; 120:584–593. [PubMed: 17766532]
5. Jeste SS, Sahin M, Bolton P, Ploubidis GB, Humphrey A. Characterization of autism in young children with tuberous sclerosis complex. J Child Neurol. 2008; 23:520–525. [PubMed: 18160549]
6. Ertan G, Arulrajah S, Tekes A, Jordan L, Huisman TA. Cerebellar abnormality in children and young adults with tuberous sclerosis complex: MR and diffusion weighted imaging findings. J Neuroradiol. 2010; 37:231–238. [PubMed: 20381146]
7. Weber AM, Egelhoff JC, McKellop JM, Franz DN. Autism and the cerebellum: evidence from tuberous sclerosis. J Autism Dev Disord. 2000; 30:511–517. [PubMed: 11261463]
8. Eluvathingal TJ, et al. Cerebellar lesions in tuberous sclerosis complex: neurobehavioral and neuroimaging correlates. J Child Neurol. 2006; 21:846–851. [PubMed: 17005099]
9. Asano E, et al. Autism in tuberous sclerosis complex is related to both cortical and subcortical dysfunction. Neurology. 2001; 57:1269–1277. [PubMed: 11591847]
10. Kwiatkowski DJ, et al. A mouse model of TSC1 reveals sex-dependent lethality from liver hemangiomas, and up-regulation of p70S6 kinase activity in Tsc1 null cells. Hum Mol Genet. 2002; 11:525–534. [PubMed: 11875047]
11. Barski JJ, Dethleffsen K, Meyer M. Cre recombinase expression in cerebellar Purkinje cells. Genesis. 2000; 28:93–98. [PubMed: 11105049]
12. Tsai P, Sahin M. Mechanisms of neurocognitive dysfunction and therapeutic considerations in tuberous sclerosis complex. Curr Opin Neurol. 2011; 24:106–113. [PubMed: 21301339]
13. Sajdel-Sulkowska EM, Xu M, Koibuchi N. Increase in cerebellar neurotrophin-3 and oxidative stress markers in autism. Cerebellum. 2009; 8:366–372. [PubMed: 19357934]
14. Di Nardo A, et al. Tuberous sclerosis complex activity is required to control neuronal stress responses in an mTOR-dependent manner. J Neurosci. 2009; 29:5926–5937. [PubMed: 19420259]
15. Reith RM, Way S, McKenna J 3rd, Haines K, Gambello MJ. Loss of the tuberous sclerosis complex protein tuberin causes Purkinje cell degeneration. Neurobiol Dis. 2011; 43:113–122. [PubMed: 21419848]
16. Nie D, et al. Tsc2-Rheb signaling regulates EphA-mediated axon guidance. Nat Neurosci. 2010; 13:163–172. [PubMed: 20062052]
17. Tavazoie SF, Alvarez VA, Ridenour DA, Kwiatkowski DJ, Sabatini BL. Regulation of neuronal morphology and function by the tumor suppressors Tsc1 and Tsc2. Nat Neurosci. 2005; 8:1727–1734. [PubMed: 16286931]

18. Meikle L, et al. A mouse model of tuberous sclerosis: neuronal loss of Tsc1 causes dysplastic and ectopic neurons, reduced myelination, seizure activity, and limited survival. J Neurosci. 2007; 27:5546–5558. [PubMed: 17522300]
19. Meikle L, et al. Response of a neuronal model of tuberous sclerosis to mammalian target of rapamycin (mTOR) inhibitors: effects on mTORC1 and Akt signaling lead to improved survival and function. J Neurosci. 2008; 28:5422–5432. [PubMed: 18495876]
20. Bateup HS, Takasaki KT, Saulnier JL, Denefrio CL, Sabatini BL. Loss of Tsc1 In Vivo Impairs Hippocampal mGluR-LTD and Increases Excitatory Synaptic Function. J Neurosci. 2011; 31:8862–8869. [PubMed: 21677170]
21. Choi YJ, et al. Tuberous sclerosis complex proteins control axon formation. Genes Dev. 2008; 22:2485–2495. [PubMed: 18794346]
22. Young DM, Schenk AK, Yang SB, Jan YN, Jan LY. Altered ultrasonic vocalizations in a tuberous sclerosis mouse model of autism. Proc Natl Acad Sci U S A. 2010; 107:11074–11079. [PubMed: 20534473]
23. Scattoni ML, Crawley J, Ricceri L. Ultrasonic vocalizations: a tool for behavioural phenotyping of mouse models of neurodevelopmental disorders. Neurosci Biobehav Rev. 2009; 33:508–515. [PubMed: 18771687]
24. De Zeeuw CI, et al. Spatiotemporal firing patterns in the cerebellum. Nat Rev Neurosci. 2011; 12:327–344. [PubMed: 21544091]
25. Ryu YH, et al. Perfusion impairments in infantile autism on technetium-99m ethyl cysteinate dimer brain single-photon emission tomography: comparison with findings on magnetic resonance imaging. Eur J Nucl Med. 1999; 26:253–259. [PubMed: 10079316]
26. Zhou J, et al. Pharmacological inhibition of mTORC1 suppresses anatomical, cellular, and behavioral abnormalities in neural-specific Pten knock-out mice. J Neurosci. 2009; 29:1773–1783. [PubMed: 19211884]
27. Insel TR, Fernald RD. How the brain processes social information: searching for the social brain. Annu Rev Neurosci. 2004; 27:697–722. [PubMed: 15217348]
28. Steinlin M. Cerebellar disorders in childhood: cognitive problems. Cerebellum. 2008; 7:607–610. [PubMed: 19057977]
29. Muller RA. The study of autism as a distributed disorder. Ment Retard Dev Disabil Res Rev. 2007; 13:85–95. [PubMed: 17326118]
30. Schmahmann JD. Disorders of the cerebellum: ataxia, dysmetria of thought, and the cerebellar cognitive affective syndrome. J Neuropsychiatry Clin Neurosci. 2004; 16:367–378. [PubMed: 15377747]
31. Yang M, Silverman JL, Crawley JN. Automated three-chambered social approach task for mice. Curr Protoc Neurosci. 2011 Chapter 8, Unit 8 26.
32. Holmes A, et al. Behavioral characterization of dopamine D5 receptor null mutant mice. Behav Neurosci. 2001; 115:1129–1144. [PubMed: 11584926]
33. Yang M, Crawley JN. Simple behavioral assessment of mouse olfaction. Curr Protoc Neurosci. 2009 Chapter 8, Unit 8 24.
34. Silverman JL, et al. Sociability and motor functions in Shank1 mutant mice. Brain Res. 2011; 1380:120–137. [PubMed: 20868654]
35. Bednar I, et al. Selective nicotinic receptor consequences in APP(SWE) transgenic mice. Mol Cell Neurosci. 2002; 20:354–365. [PubMed: 12093166]
36. Kurejova M, et al. An improved behavioural assay demonstrates that ultrasound vocalizations constitute a reliable indicator of chronic cancer pain and neuropathic pain. Mol Pain. 2010; 6:18. [PubMed: 20346101]
37. Buitrago MM, Schulz JB, Dichgans J, Luft AR. Short and long-term motor skill learning in an accelerated rotarod training paradigm. Neurobiol Learn Mem. 2004; 81:211–216. [PubMed: 15082022]
38. Hull C, Regehr WG. Identification of an inhibitory circuit that regulates cerebellar Golgi cell activity. Neuron. 2012; 73:149–158. [PubMed: 22243753]

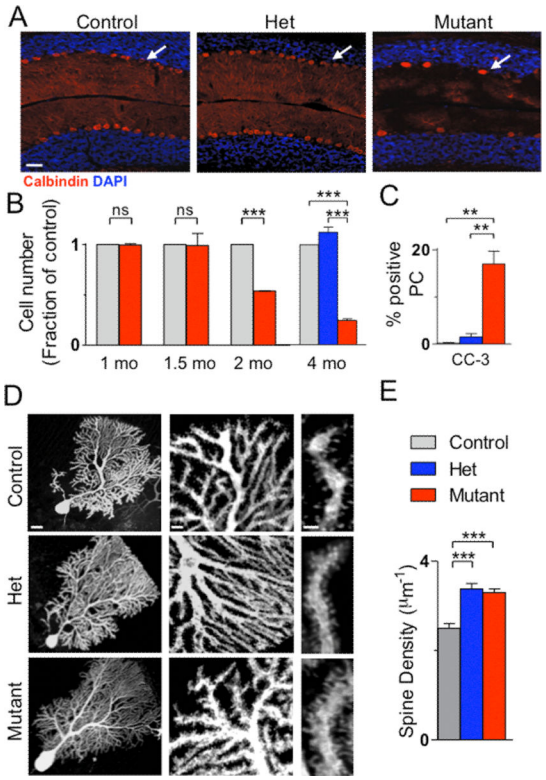

Figure 1. PC *Tsc1* mutants display reduced PC numbers and abnormal PC morphology

A. Mutants displayed reduced Purkinje cell numbers by Calbindin staining. **B**. PC loss occurred by 2 months in mutants. No PC loss was observed in hets at 4 months. **C**. Increased cleaved caspase-3 (CC-3) staining in mutants. (for B-C, controls/mutants: n=3 mice; hets, n=2 mice; >500 cells/group) **D., E**. Mutant PCs displayed increased spine density. (control: n=10 cells, 3 mice; het: n=10 cells, 4 mice; mutant: n=11 cells, 3 mice). *** $p < 0.001$, two-way ANOVA, Bonferroni's post hoc analysis. Scale bars in A.100μm; D. 20μm (left), 5μm (middle), 2μm (right).

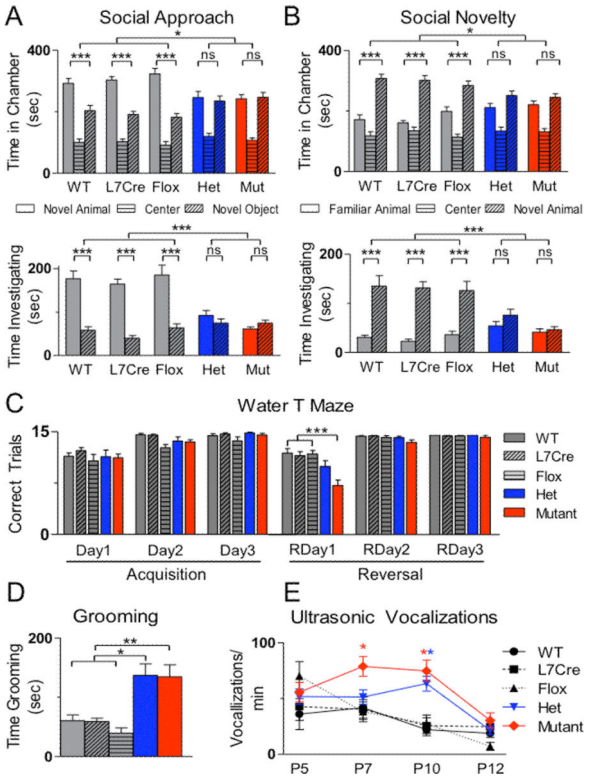

Figure 2. PC *Tsc1* hets and mutants display autistic-like behaviors

A. In assays of social approach, unlike all control genotypes (WT, L7Cre, and Flox), hets and mutants (mut) demonstrated no significant preference for novel mouse over novel object by time spent in chamber (above) or time in close interaction (below) with novel mouse. **B**. Unlike controls, hets and mutants also failed to display preference for social novelty in chamber (above) and close interaction (below) times. n≥11 for each group. **C**. Mutants displayed normal acquisition of escape platform location but impairments on day 1 of reversal learning (RDay) 1 in a water T-maze. (total trials = 15), n≥13 for each group. **D**. Hets and mutants spent significantly more time self-grooming. n≥11 for each group. **E**. Hets (P10) and mutants (P7, 10) pups emitted significantly more ultrasonic vocalizations than controls. n≥8 for each time point and group. ns, $p>0.05$; *, $p<0.05$; ** $p<0.01$, *** $p<0.001$, two-way ANOVA, Bonferroni's post hoc analysis.

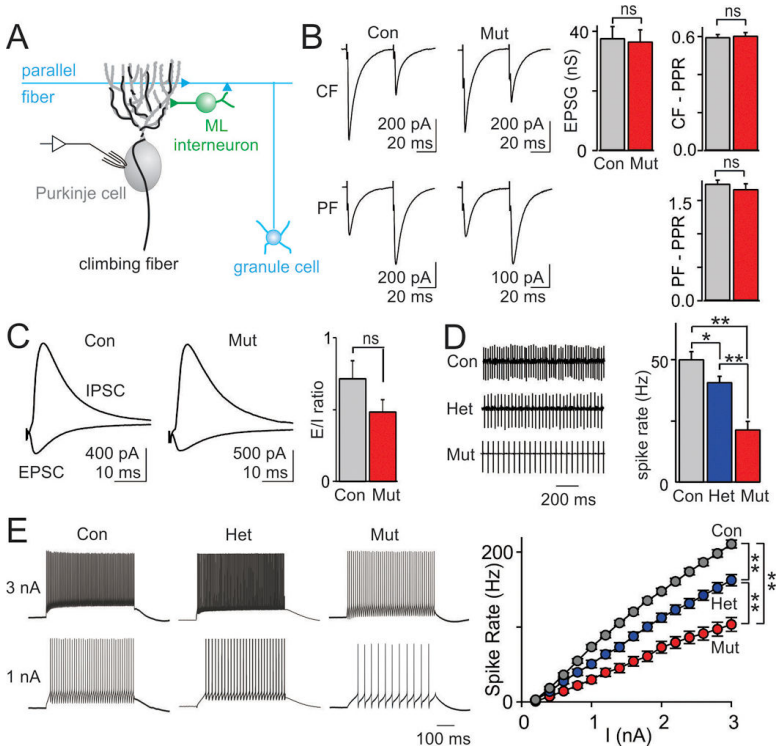

Figure 3. PC excitability is reduced in PC *Tsc1* hets and mutants, but no significant difference in synaptic inputs to PCs is apparent

A. Schematic of the electrophysiological recording configuration and synaptic inputs onto cerebellar PCs. **B**. Electrical stimulation of climbing fibers (CF, top) and granule cell-mediated parallel fiber (PF, bottom). Whole cell mode voltage-clamp recordings showed no difference in the conductance (g) of single fiber CF inputs (control (con) n=20 cells, 5 mice; mutant (mut) n=16 cells, 5 mice, p=0.34), or the paired-pulse ratio (PPR) of either CF or PF inputs (CF PPR: con n=8, mut n=5, p=0.51). **C**. Electrical stimulation revealed no differences in the ratio of evoked synaptic excitation to inhibition (E/I ratio; con n=29, mut n=17, p=0.19). **D**. Extracelluar recording of spontaneous PC spiking (left) revealed a significantly lower spike rate in hets and mutants (right, con n=77 cells, 12 mice, het n=62 cells, 7 mice; n=42 cells, 9 mice). **E**. Whole cell mode current-clamp recordings showed reduced excitability in PCs from hets and mutants compared to control PCs. *Left*, current injections of 1 and 3 nA produced fewer spikes in PCs from hets and mutants. *Right*, average data showed a reduced spike output for mutant PCs (con n=77 cells, 12 mice, het n=48 cells, 7 mice; n=43 cells, 9 mice). ns, p>0.05, * p<0.05, ** p<0.01. two-way ANOVA, Bonferroni's post hoc analysis.

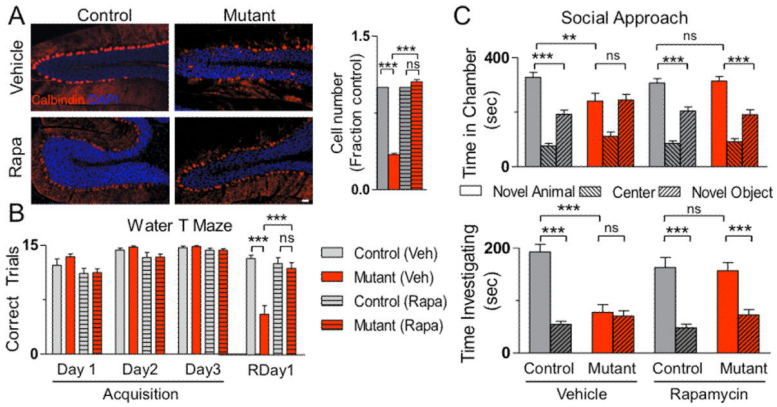

Figure 4. Rapamycin treatment prevents pathologic and behavior abnormalities in PC *Tsc1* mutant mice

A. Treatment with rapamycin (Rapa) prevented cell loss seen in vehicle (Veh) treated PC *Tsc1* mutants. Scale bar: 100 μm. Quantification of cell numbers on right (n > 500cells; 2 mice per group) **B., C**. Whereas vehicle treated mutants displayed behavioral deficits, rapamycin treated mutants displayed amelioration of these deficits in **B**. reversal learning in the water T maze (n≥9 in each group) and in **C**. social approach in the three chambered apparatus (n≥10). As behavioral phenotypes were not significantly different between the three control genotypes in untreated mice, control genotypes were pooled into a single group for these studies. ns, $p>0.05$; *, $p<0.05$; *** $p<0.001$, two-way ANOVA, Bonferroni's post hoc analysis.